J Mater Sci (2012) 47:711–719
DOI 10.1007/s10853-011-5844-6

Synthesis and characterization of carbon hollow microspheres

Quan Jin · Mingtao Zheng · Yongjian Wu · Chunlin Xie · Yong Xiao · Yingliang Liu

Received: 27 June 2011 / Accepted: 2 August 2011 / Published online: 18 August 2011

Abstract A facile approach was developed for synthesis of carbon hollow microspheres (CHM) via carbonization of the hollow polymer microspheres prepared from polymerization in the presence of L-lysine acted as in situ template. The physical and chemical structures of the samples were investigated by X-ray powder diffraction, Raman spectrum, scanning electron microscopy (SEM), and transmission electron microscopy (TEM). SEM and TEM images show that the products consist of a large scale of monodisperse CHM with a size of about 1.1–1.3 μm. Furthermore, the resulting CHMs possess a surface area of 559 $m^2\ g^{-1}$ and a pore volume of 0.27 $cm^3\ g^{-1}$. The morphology and the size of the as-obtained samples can be controlled by the polymerization temperature, polymerization time, and the dosage of L-lysine. Moreover, a possible formation mechanism of the CHM has been put forward according to the experimental data available.

Introduction

In recent years, carbon materials are of particular interest due to their distinctive functions, novel properties, and potential applications in advanced devices and biotechnologies. Many types of carbon materials have been synthesized, such as carbon spheres [1–4], carbon hollow microspheres (CHM) [5, 6], carbon hollow cones (CHC) [7], carbon nanotubes (CNT) [8–10], carbon nanocables (CNC) [11], carbon straw-like microbundles (CSM) [12], flower-like carbon [13], and so on. Among them, CHM have attracted growing research interest owing to their excellent properties such as low density, high specific surface area, high damping characteristics, good chemical stability, and available hollow interiors, which make them technologically important in a wide range of potential applications in lithium–ion batteries [14], catalysis supports [15], supercapacitors [16], hydrogen storage [17], drug delivery [18], and so on. This promise has motivated intense research efforts seeking to develop special and general routes for synthesizing CHM. The hard template method is probably the most effective and general method for CHM. For instance, monodisperse silica spheres are usually used as hard templates, because they are readily available in a wide range of sizes [19]. However, the synthesis procedure is complicated and time consuming, since the hard templates must be synthesized beforehand and introduce the carbon precursor on the template by liquid impregnation or by gas-phase chemical vapor deposition. Consequently, other approaches have been reported to synthesize CHM, such as arc discharge approach [11], hydrothermal reduction [12] etc. Liu et al. [20] synthesized CHM with CCl_4 as carbon source in a stainless autoclave. Our group [21] had synthesized CHM by pyrolysis of absolute ethanol and zinc acetate with the same approach. Nevertheless, the disadvantages of these ways to prepare CHM are not easily controlled, and the morphology or the size of the products was nonuniform.

Recently, carbonization of hollow organic polymer offers an attractive method for fabricating CHM. This approach is much simpler than conventional ones involving separate procedures for preparation of template materials. Zhang et al. [22] synthesized CHM via carbonization of the

Electronic supplementary material The online version of this article (doi:10.1007/s10853-011-5844-6) contains supplementary material, which is available to authorized users.

Q. Jin · M. Zheng · Y. Wu · C. Xie · Y. Xiao · Y. Liu (✉)
Department of Chemistry and Institute of Nanochemistry, Jinan University, Guangzhou 510632, People's Republic of China
e-mail: tliuyl@jnu.edu.cn

resorcinol formaldehyde (RF) hollow particles by an inverse-emulsion system. Lu et al. [23] have fabricated CHM through carbonizing hollow polymer microsphere (HPS) prepared by this approach. However, it usually needs expensive surfactants for controlling the morphology of the HPS, and it is difficult to control the size of the products, thus confined the preparation and applications of the CHM. Consequently, there remains still a challenge as to developing a simple and none-surfactants way for synthesizing morphology and size-controlled CHM.

Herein, we demonstrated a facile approach without using surfactants for preparing monodispersed CHM on a large scale via carbonization of HPS. The obtained samples displayed a surface area of 559 m^2 g^{-1} and a pore volume of 0.27 cm^3 g^{-1}. In addition, the polymerization temperature, the polymerization time, and the dosage of the L-lysine were investigated. We found that the morphology and the size of the CHM can be controlled by these reaction conditions. Furthermore, this article also discussed the possible formation mechanism of the CHM.

Experimental section

Chemicals

All reagents were commercially available and used without further purification. 2,4-Dihydroxybenzoic acid (A.R. grade) and L-lysine (A.R. grade) were purchased from Aladdin. Formaldehyde (37%) and absolute ethanol were obtained from Tianjin Damao Chemical Reagent Factory.

Synthesis of CHM

In a typical synthesis of the CHM, 1.54 g of 2,4-dihydroxybenzoic acid (10 mmol) and 0.48 g of L-lysine (3 mmol) were dispersed in 300 mL absolute ethanol in a three-necked flask, and the system kept refluxing at 80 °C with vigorously stirring for 2–4 h under nitrogen protection. After a homogenous solution was obtained, 1.62 g of formaldehyde (20 mmol) was added into the system and kept stirring and refluxing. After 24 h, the precipitate was filtered, washed with ethanol several times to wash the residue, then dried in a vacuum at 60 °C for 6 h to get the core–shell microspheres. After this step, the as-obtained core–shell microspheres were washed with water several times (this step is crucial, to obtain the HPS), then dried in a vacuum at 60 °C for 6 h. The HPS was put into an electronic furnace, which was then heated to 800 °C with a heating rate of 1 °C min^{-1} and maintained at this temperature for 2 h under nitrogen protection. In order to disclose the effect of polymerization temperature, it was controlled at 70, 80, 90, and 100 °C while keeping the other reaction conditions constant. The polymerization reaction time was regulated for 36, 24, 12, and 6 h to investigate its influence on the shell thickness of the products. To obtain the tunable particle size of the CHM, dosage of L-lysine varied in the range of 0.48–0.12 g.

Characterization

Structural characterization was performed by using X-ray powder diffraction (XRD) (Brucks D8 X-ray powder diffractometer, Cu Kα radiation, 40 kV, 20 mA, $k = 1.541874$ Å). FT-IR spectra were measured by an Equinox 55 (Bruker) spectrometer with the KBr pellet technique ranging from 500 to 4000 cm^{-1}. The morphologies of the samples were characterized with scanning electron microscopy (SEM, Philips XL-30 s) and transmission electron microscopy (TEM, Philips Tecnai-10). The Raman spectrum was recorded at room temperature on a Renishaw RM2000 Raman microspectrometer with the 514.5 nm line of an argon laser. The specific surface areas were determined from nitrogen adsorption using the Brunauer–Emmett–Teller (BET) equation. The total pore volume was determined from the amount of gas adsorbed at the relative pressure of 0.99. Micropore (pore size <2 nm) volume of the CHM was calculated from the analysis of the absorption isotherm using the Horvath–Kawazoe (HK) method. Pore size distribution (PSD) was derived from the analysis of the adsorption branch using the Barrett–Joyner–Halenda (BJH) method.

Results and discussion

Morphology and structure of the CHMs

A typical XRD pattern of the as-synthesized CHM obtained from carbonizing the HPS synthesized at 80 °C for 24 h with 0.48 g L-lysine is shown in Fig. 1a. There is a broad peak at 26° that corresponds to the (002) plane of graphite. In addition, a small shoulder peak at 43.1°, corresponding to the (101) plane of graphite, can be observed. The broadening of the two peaks suggests the possible presence of an amorphous carbon phase within the CHM [3, 24]. No other impurity is observed in the XRD pattern. The Raman spectrum is also used to further analyze the molecular structure of the CHM. Figure 1b shows the micro-Raman spectrum of the sample. There are two broad peaks in the image. One band is located around 1340 cm^{-1} (D-band; the defects within the carbon) and the other is around 1580 cm^{-1} (G-band; the interplane sp^2 C–C stretching), also indicating the amorphous carbon structure. It is known that the graphitization degree of carbons can be confirmed by the width of the I_G peak and the value of I_D/I_G.

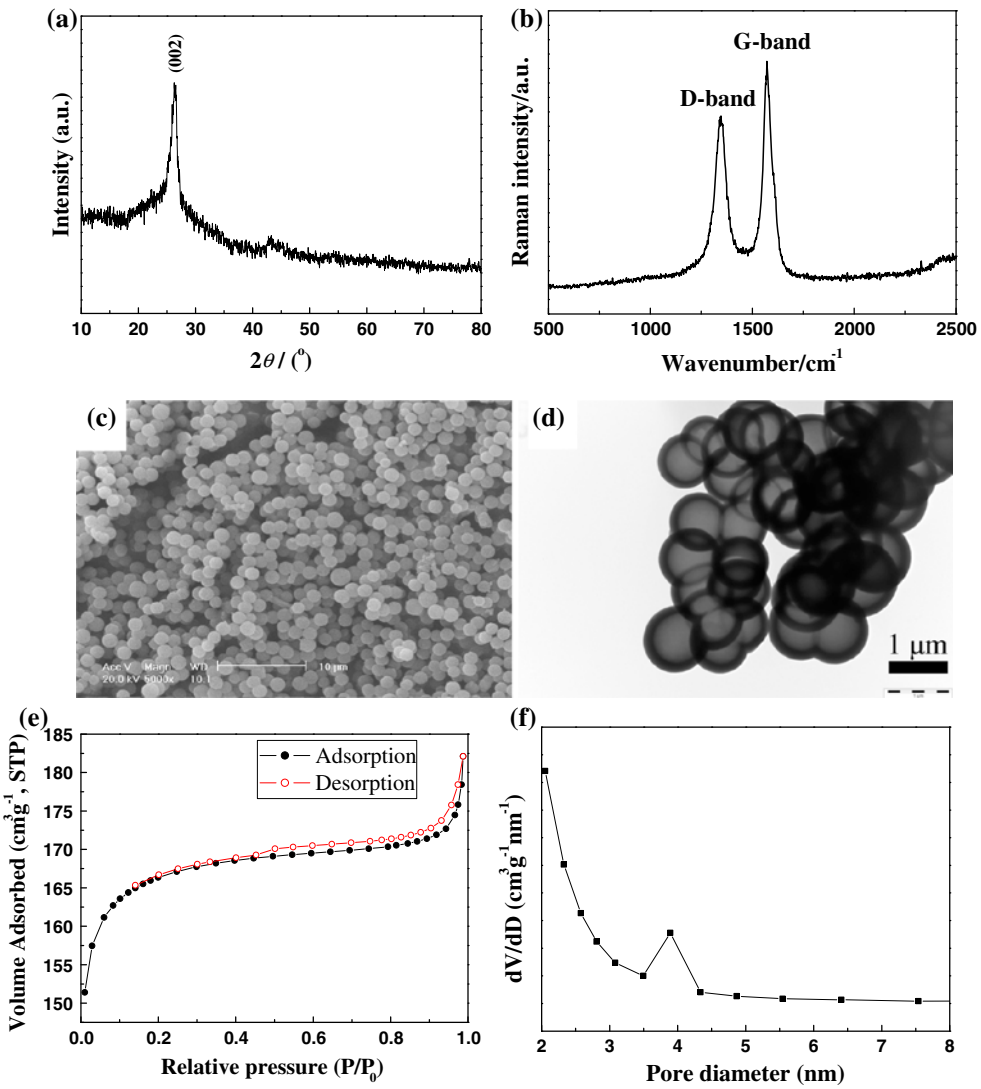

Fig. 1 **a** XRD patterns, **b** Raman spectrum, **c** SEM image, **d** TEM image, **e** adsorption–desorption isotherms, and **f** PSD of the as-prepared CHM

The relatively large I_D/I_G indicates the lower graphitization degree in the resultant CHM [21], in agreement with the XRD result.

SEM and TEM are employed to observe the morphology of the sample. Representative images of the morphology of the sample are shown in Fig. 1c, d. The SEM image (Fig. 1c) reveals that the morphology of samples is microspheres with average diameter of about 1.1–1.3 μm. It can also be seen in Fig. 1c that there are no other products, such as CNTs and carbon fibers, suggesting the high purity of the product. The hollow nature of the CHM is confirmed by the TEM image (Fig. 1d), which shows the as-lighter contrast in the center, verifying the microspheres are hollow structure. The darker contrast of the rims would correspond to the shells of the microspheres, the thickness of these walls being around 120–140 nm.

The porosity of the obtained CHM is investigated by nitrogen adsorption–desorption isotherms (Fig. 1e, f). A part of the pore size is less than 2.0 nm and the other is as 3.8 nm estimated from the PSD. The sample exhibited a high surface area of 559 $m^2\ g^{-1}$ (micropore area: 499 $m^2\ g^{-1}$; external surface area: 60 $m^2\ g^{-1}$) and a total pore volume of 0.27 $cm^3\ g^{-1}$, which are mainly attributable to the presence of the nanopores in the shell (micropore volume: 0.23 $cm^3\ g^{-1}$). The micropore area of CHM is much larger than the external surface area, which makes the CHM an ideal candidate for hydrogen storage.

Polymerization process of the polymer precursors

Effect of the polymerization temperature

Among the factors of polymerization temperature, polymerization reaction time and dosage of L-lysine, temperature has influence on the morphology and size of the final products. We regulated the polymerization temperature and

kept other conditions constant. When the polymerization temperature used in this study was at 70 °C, for it was not high for the polymerization reaction, resulted in reduction of the product. Figure 2a, b displayed that the morphology and size of CHM was not distinct from the CMH obtained at 80 °C, but the yield of the products decreased. If enhanced the polymerization temperature to 90 °C, hollow spherical particles with nonuniform size (0.5–2 μm) were obtained (Fig. 2c, d). Figure 2e is the SEM image of sample obtained at 100 °C, displaying that the product is composed of spherical particles with the average diameter as the sample obtained at 90 °C and there are a few nanotube-like products (indicated with a black arrow). Figure 2f is the TEM image of the sample obtained at 100 °C, some hollow tube-like morphology (displayed with a black arrow) can be seen, in accordance with SEM results above. With the set of experiments of the polymerization temperature, we proposed that the uniform morphology and size of CHM could be synthesized at relatively stable reaction system. However, if the polymerization temperature reached to 90 °C that is far beyond the boiling point of ethanol (78.4 °C), ethanol maintains boiling all the time during the whole polymerization reaction, which leads to different size distributions. What is more, when the polymerization temperature was added to higher temperature, such as 100 °C, the system was more unstable and the polymerization rate was greatly improved, resulting in a few other morphologies, such as nanotube-like products. Consequently, the appropriate polymerization temperature to synthesize CHM with uniform morphology, same size and in a suitable yield is at 80 °C.

Effect of the polymerization time

In order to investigate the role of the polymerization time, a series of experiments have been done. Figure 3a–f gives the SEM and TEM images of the samples obtained for 36, 12, and 6 h. Comparing the images in Fig. 3b and in Fig. 1d, we have found that with the increase of the

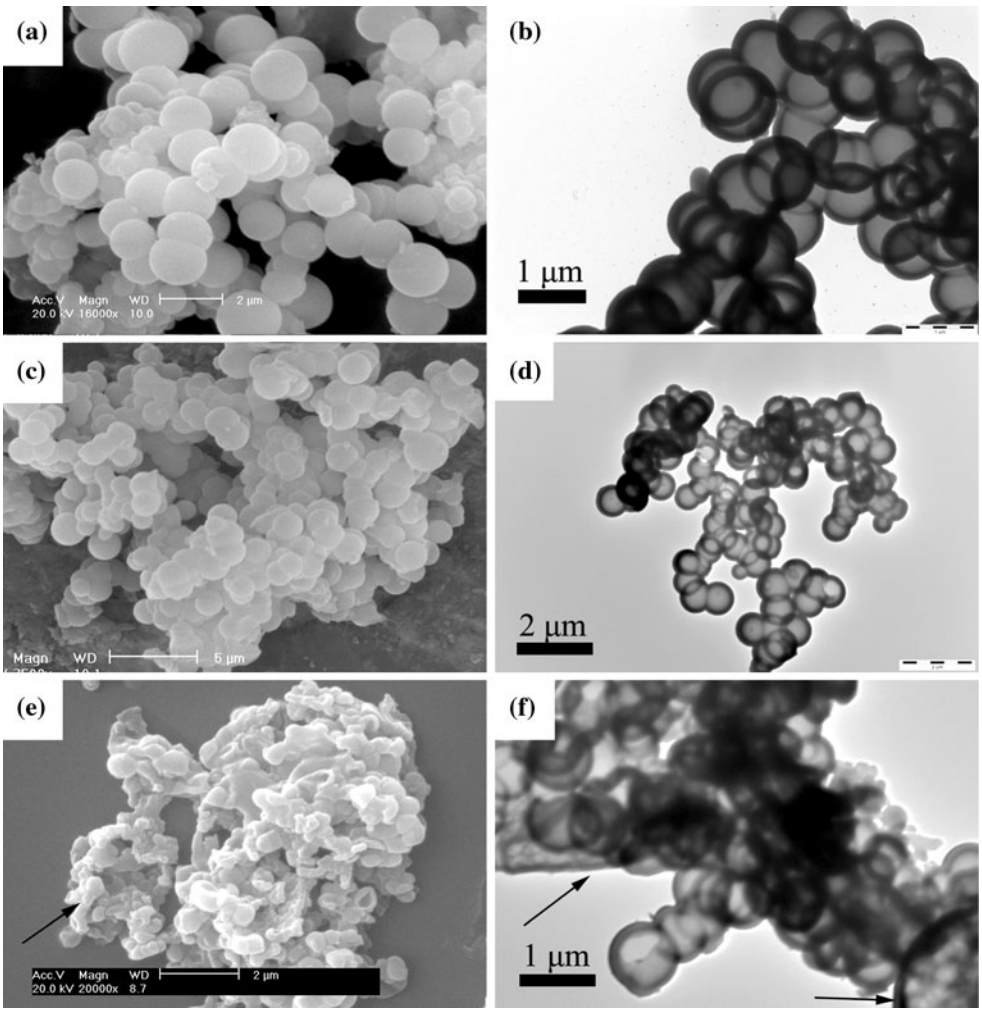

Fig. 2 SEM and TEM images of the samples obtained at different temperature for 24 h: **a**, **b** 70 °C, **c**, **d** 90 °C, and **e**, **f** 100 °C

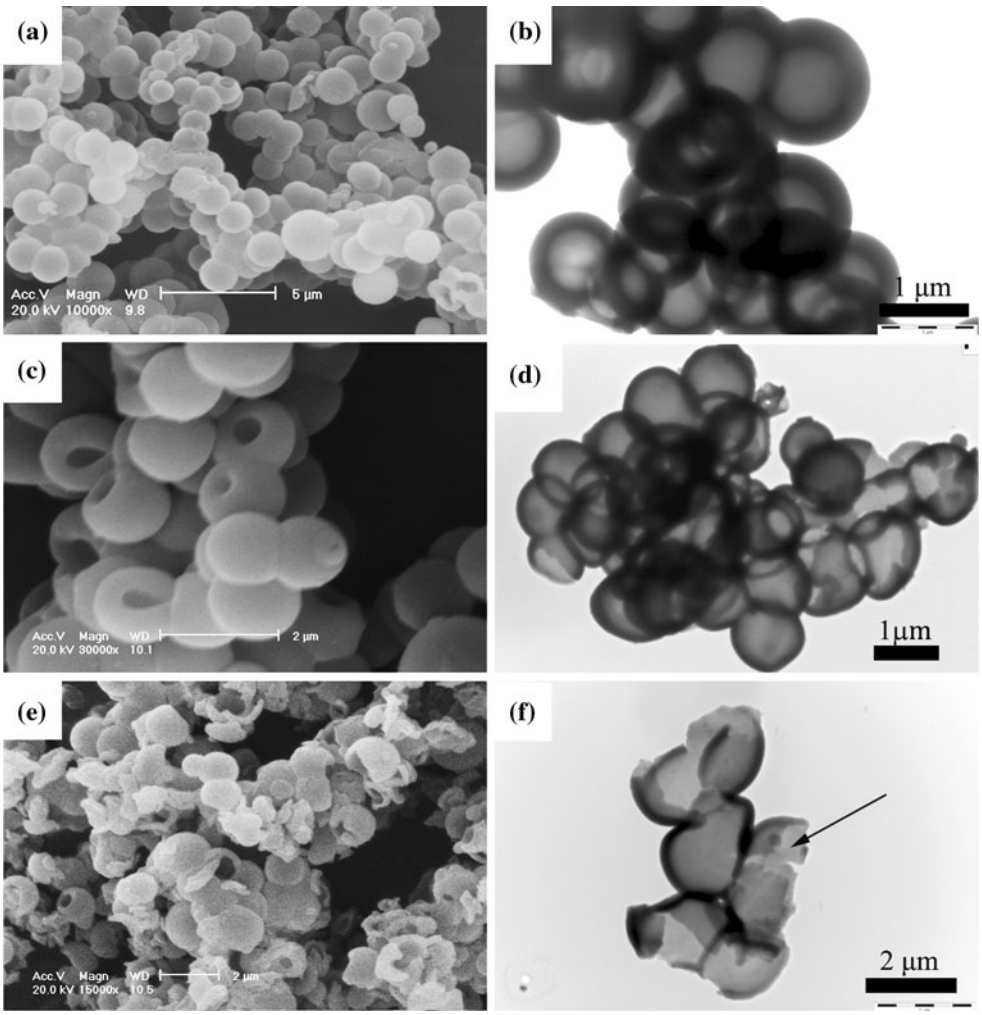

Fig. 3 SEM and TEM images of the products synthesized at 80 °C for different times: **a**, **b** 36 h, **c**, **d** 12 h, and **e**, **f** 6 h

polymerization time, the shell thickness of the CHM increases from 120–140 to 160–180 nm. However, the dispersibility is not as good as the sample obtained for 24 h. On the contrary, in a short reaction time of 12 h, the average shell thickness of the CHM ranges from 100 to 120 nm, indicating that the shell thickness of the hollow spheres decreased with the decrease of the polymerization time, as shown in Fig. 3d. It is notable that some hollow bowl-like capsules can be observed in Fig. 3c, according to the TEM image in Fig. 3d. As the polymerization time decreased to 6 h, the resultant products at this stage appear to be easily collapsed, resulting in a large number of broken hollow spheres and even some of them changed into pieces, which can be seen in Fig. 3e. It can also be observed from Fig. 3f that there are a number of cracks on the sample (displayed with a black arrow) with shell thicknesses from 60 to 80 nm, verifying the occurrence of the collapse. It occurred due to the pressure difference caused by the occurrence of capillary forces during drying [25]. With the set of experiments, the results show that polymerization time plays a vital role in the formation of CHM, and 24 h is selected as the optimum condition.

Effect of the dosage of the L*-lysine*

It was found that the concentration of the L-lysine plays a crucial role in controlling the diameter and size distribution of the products. Figure 4a–f shows the SEM and TEM images of the products prepared from the synthesis system with different concentration L-lysine, such as 0.48, 0.24, and 0.12 g. It can be observed that the average size of the spheres is about 1.2, 0.9, and 0.6 μm, respectively. The morphology and the size of the samples are uniform, and no other products exist, revealing that the size of the CHM tends to decrease with the decrease of the concentration of the L-lysine. In addition, the dispersibility of the CHM obtained from different dosages of the L-lysine is good. It is worth noting that the shell thicknesses of all the three types

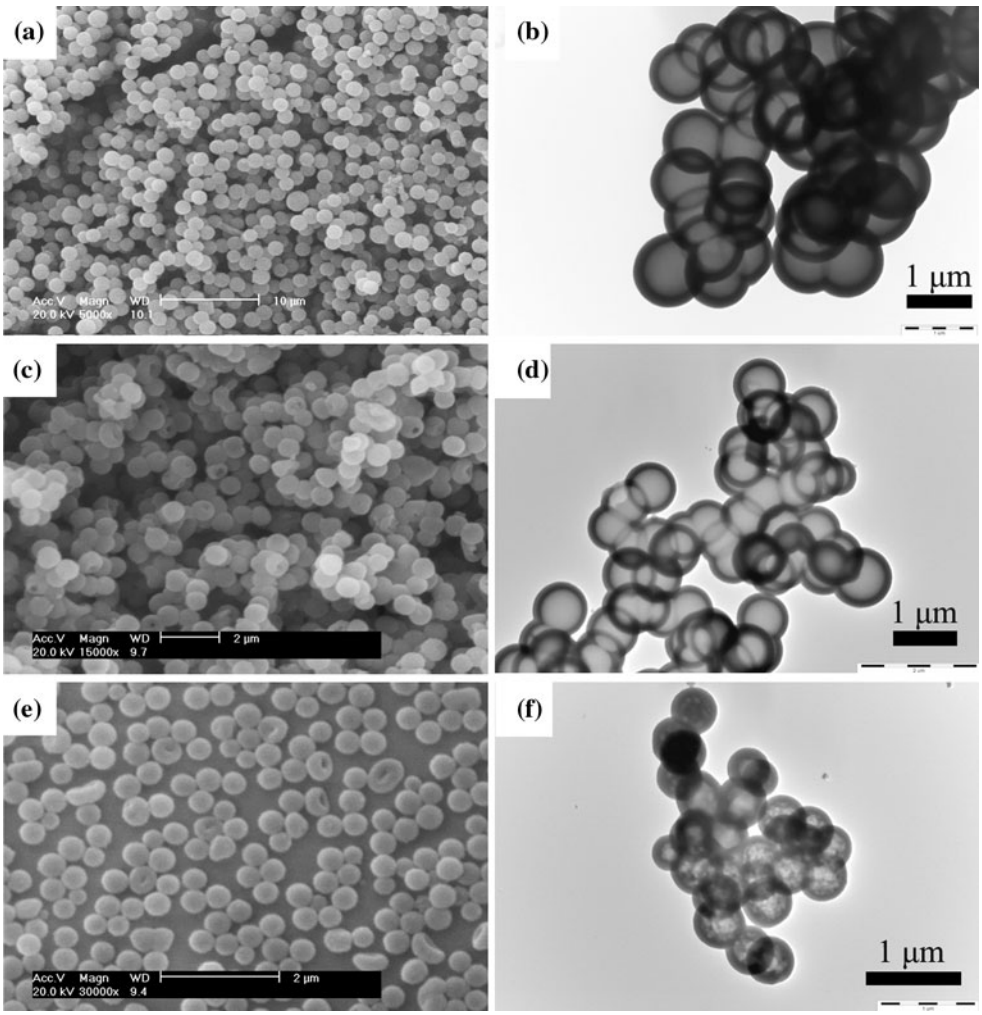

Fig. 4 SEM and TEM images of the samples prepared at 80 °C for 24 h with different amounts of L-lysine: **a**, **b** 0.48 g, **c**, **d** 0.24 g, and **e**, **f** 0.12 g

of the CHMs are approximate 120–140 nm (Fig. 4b, d, and f). These results indicate that the size of the CHM can be regulated by the concentration of the L-lysine. It is possible that a kind of in situ template is formed from L-lysine during the polymerization, and the size of the in situ templates depend on the concentration of the L-lysine, leading to the products with different average diameters. We will give a further discussion in the mechanism section [21].

Formation mechanism of the CHM

In order to understand the formation mechanism of the CHM, it is necessary to study the formation mechanism of the HPS, because the CHM can be easily obtained by carbonizing the HPS. To discuss the formation of the HPS, we collected the polymer only washed by ethanol to remove residual reactant, and the samples without washing with water. The TEM image in Fig. 5a displays the polymer obtained at 80 °C for 24 h with 0.12 g L-lysine, and we can only observe core/shell microspheres in the picture, exhibiting that both the core and shell of the sample are stable in ethanol. The SEM image of the sample is shown in Fig. 5b, we can clearly see from the image that there are some broken microspheres with core/shell structure (the core displayed with a white arrow), corresponding to the TEM results. It is worthy to note that without using L-lysine, the morphology of the as-obtained sample is disordered and no core/shell microspheres can be gained (Fig. S1, Supporting Information). In addition, besides L-lysine, other amino acids such as L-asparagine, L-tryptophan, L-serine, and L-leucine were also used for the preparation of HPS. Following the best synthesis conditions of sample obtained at 80 °C for 24 h, the amount of the amino acids were 3 mmol. However, there were only solid microspheres. It showed that using L-asparagine, L-tryptophan, L-serine, and L-leucine are able to act as the polymerization initiators, but unable to as template to form

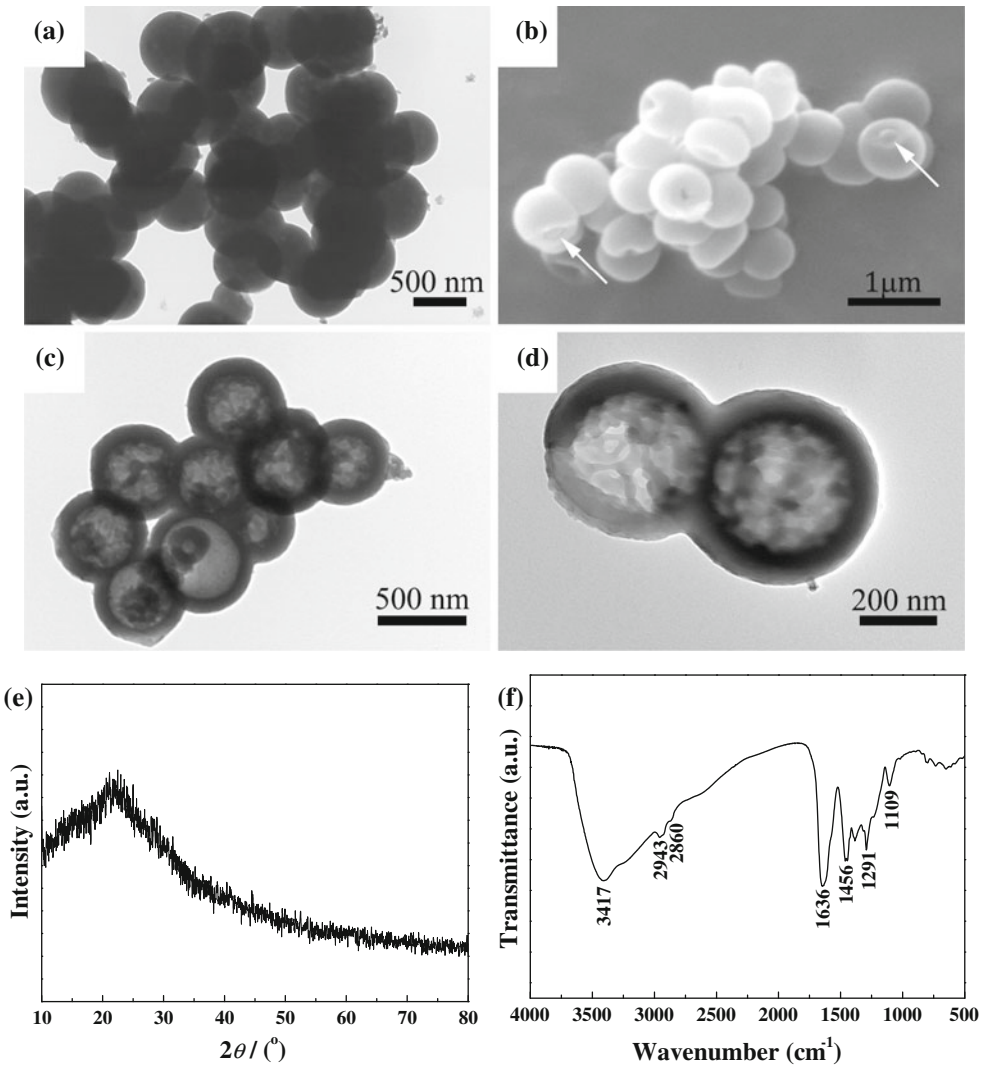

Fig. 5 **a**, **b** TEM and SEM images of the poly(L-lysine)/phenolic resin core/shell, **c** TEM image at low magnification, **d** magnified TEM image shows the details of the HPS, **e** XRD patterns, and **f** FT-IR spectra of the as-obtained of the HPS

core/shell microspheres in the resultant polymers. It can be inferred from these results that L-lysine is unique for the synthesis of the core/shell microspheres.

More interestingly, after the core/shell microspheres were washed with water, filtered, and dried, HPS can be obtained. The TEM image (Fig. 5c, d) shows the microspheres are hollow structure, meaning that the core has been completely eliminated. The darker contrast of the rims refers to the shells of the hollow microspheres, demonstrating that the core of the core/shell microspheres is easily dissolved with water and removed to obtain HPS, while the shell can not be dissolved, which suggests that the shell is stable in ethanol and water.

To investigate the composition of the shell of the HPS, it was characterized by XRD and FT-IR. Figure 5e gives its XRD patterns. It exhibits that one broad peak at 2θ of 24° and deviate the peak at around 26° that could be attributed to the (002) diffraction planes. It states clearly the

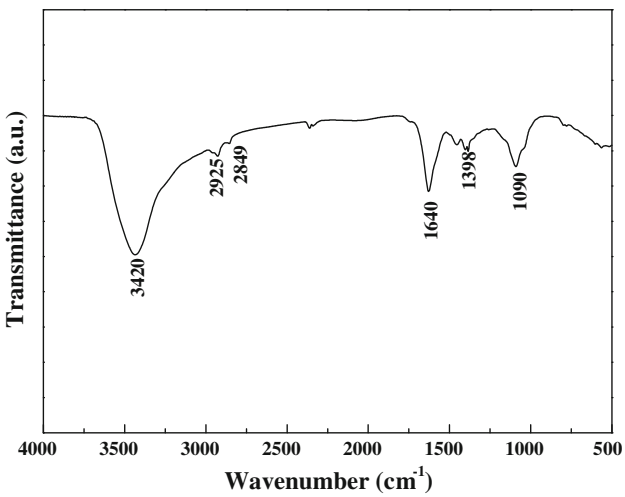

Fig. 6 FT-IR spectra of the filtrate from the poly(L-lysine)/phenolic resin core/shell washed with water

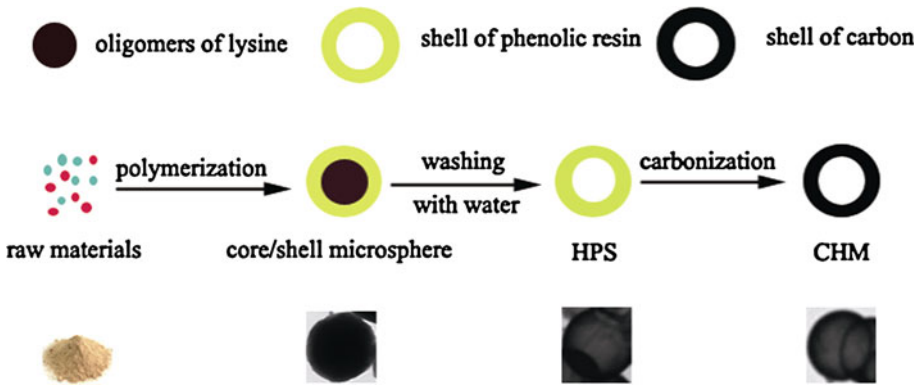

Fig. 7 Schematic representation of the possible formation mechanism of the CHM

carbonization degree of the sample is very low. Figure 5f is the FT-IR spectroscopy of the HPS. It reveals that the strong characteristic peak at 3417 cm^{-1} is attributed to the O–H stretching vibration [26], implying that there are hydroxyl groups on the sample. The absorption peak at 1636 cm^{-1} corresponds to the stretching vibration of carboxyl group. The peaks at 1456 and 1109 cm^{-1} are due to the stretching vibration of phenyl group and C–O [4], respectively. The infrared spectrum peaked at 2943, 2860, and 1291 cm^{-1} originate from the stretching vibration of methyl, methylene, and C–H [4]. Because, the HPS is washed with ethanol and water several times, there are on other impurities with the HPS. Combined with these results, it shows that the HPS is a kind of polymer-like phenolic resin.

It is well known that poly(amino acid) are important classes of biodegradable polymers, referring to a small group of polyamides that consist of lysine linked by amide bonds. Poly(L-lysine) is an unusual cationic, naturally occurring homopolyamide made of L-lysine, having amide linkage between e-amino and a-carboxyl groups. It is vital that poly(L-lysine) can be dissolved in water but not in ethanol, which possibly makes it as a template to obtain hollow structure. On the other hand, L-lysine molecules often changes into intra-molecule salt, so the deprotonated carboxyl group and the protonated NH_3^+ group can form hydrogen bonds with the –COOH group of 2,4-dihydroxybenzoic acid, which contributed to form polymer. So, we inferred that the core may consist of poly(L-lysine) from L-lysine during the polymerization. To determine the composition of the core, the filtrate from the polymer microspheres washed with water was collected, and then characterized by FT-IR spectroscopy. As seen from Fig. 6, the spectrum of the filtrate exhibits strong bands at 3420 cm^{-1} implying hydroxyl groups. The other strong peak at 1640 cm^{-1} is due to the stretching vibration of N–H [27]. The peak at 1090 cm^{-1} results from the stretching vibration of C–O. The band at 1398 cm^{-1} is designated as methyl C–H bending [28], and the two bands at 2925 and 2849 cm^{-1} are allocated as C–H stretching [27]. It suggests that a kind of poly(amino acid) made up of L-lysine is present in the filtrate, indicating that the core may be composed of poly(L-lysine) [27]. Therefore, it is not complicated to understand that the poly(L-lysine)/phenolic resin core/shell polymer microspheres were obtained during the polymerization.

Based on all the results above, the formation mechanism of these CHM is proposed and schematically shown in Fig. 7. In the first step, poly(L-lysine)/phenolic resin core/shell polymer microspheres are generated followed by polymerization of raw materials. In the second step, removal of the core by water etching results in the formation of HPS. Finally, CHM can be obtained by carbonizing the as-obtained HPS.

Conclusion

In summary, we have synthesized CHM by a facile approach. L-lysine plays an essential role in the formation of CHM. The particle size, shell thickness, and morphology of the CHM depend on the reaction conditions, such as polymerization temperature, polymerization time, and the dosage of the L-lysine. A possible schematic illustration was put forward to explain the formation mechanism of the CHM. The CMS may greatly widen their potential applications in biochemistry, drug delivery, catalyst support, microreactor, and so on.

Acknowledgements This study was financially supported by the Natural Science Union Foundations of China and Guangdong Province (U0734005), National Nature Science Foundation of China (20906037 and 21031001), and the Fundamental Research Funds for the Central Universities (21610102).

References

1. Koprinarov N, Konstantinova M (2011) J Mater Sci 46:1494. doi: 10.1007/s10853-010-4951-0
2. He WQ, Xiao Y, Cheng JL, Wei GD, Zhao SA, Yi GG, Liu YL (2011) J Mater Sci 46:1844. doi:10.1007/s10853-010-5011-5

3. Fan YT, Liu GH, Liu XG, Xu BS (2006) J Mater Sci 41:5242. doi:10.1007/s10853-006-0250-1
4. Zheng MT, Liu YL, Xiao Y, Zhu Y, Guan Q, Yuan DS, Zhang JX (2009) J Phys Chem C 113:8455
5. Katcho NA, Urones-Garrote E, Avila-Brande D, Gomez-Herrero A, Urbonaite S, Csillag S, Lomba E, Agullo-Rueda F, Landa-Canovas AR, Otero-Diaz LC (2007) Chem Mater 19:2304
6. Liu BY, Jia DC, Shao YF, Rao JC (2009) Mater Chem Phys 114:391
7. Gogotsi Y, Dimovski S, Libera JA (2002) Carbon 40:2263
8. Bonadiman R, Lima MD, de Andrade MJ, Bergmann CP (2006) J Mater Sci 41:7288. doi:10.1007/s10853-006-0938-2
9. Oliphant CJ, Arendse CJ, Malgas GF, Motaung DE, Muller TFG, Halindintwali S, Julies BA, Knoesen D (2009) J Mater Sci 44:2610. doi:10.1007/s10853-009-3341-y
10. Zhang XX, Deng CF, Xu R, Wang DZ (2007) J Mater Sci 42:8377. doi:10.1007/s10853-007-1941-y
11. Xi GC, Zhang M, Ma D, Zhu YC, Zhang HB, Qian YT (2006) Carbon 44:734
12. Xiao Y, Liu YL, Mi YZ, Yuan DS, Zhang JX, Cheng LQ (2005) Chem Lett 34:1422
13. Xiao Y, Liu YL, Cheng LQ, Yuan DS, Zhang JX, Gu YL, Sun GH (2006) Carbon 44:1589
14. Lee KT, Jung YS, Oh SM (2003) J Am Chem Soc 125:5652
15. Ng YH, Ikeda S, Harada T, Higashida S, Sakata T, Mori H, Matsumura M (2007) Adv Mater 19:597
16. Zhang FB, Li HL (2006) Mater Chem Phys 98:456
17. Wu CZ, Zhu X, Ye LL, OuYang CZ, Hu SQ, Lei LY, Xie Y (2006) Inorg Chem 45:8543
18. White RJ, Tauer K, Antonietti M, Titirici MM (2010) J Am Chem Soc 132:17360
19. Huang CW, Hsu CH, Kuo PL, Hsieh CT, Teng HS (2011) Carbon 49:895
20. Liu JW, Shao MW, Tang Q, Chen XY, Liu ZP, Qian YT (2003) Carbon 41:1682
21. Zheng MT, Liu YL, Zhao SA, He WQ, Xiao Y, Yuan DS (2010) Inorg Chem 49:8674
22. Zhang HJ, Ye F, Xu HF, Liu LM, Guo HF (2010) Mater Lett 64:1473
23. Lu AH, Li WC, Hao GP, Spliethoff B, Bongard HJ, Schaack BB, Schuth F (2010) Ang Chem Int Ed 49:1615
24. Xu S, Yan XB, Wang XL, Yang SR, Xue QJ (2010) J Mater Sci 45:2619. doi:10.1007/s10853-010-4239-4
25. Zoldesi CI, van Walree CA, Imhof A (2006) Langmuir 22:4343
26. Li Z, Deng Y, Wu Y, Shen B, Hu W (2007) J Mater Sci 42:9234. doi:10.1007/s10853-007-1897-y
27. Shih IL, Shen MH, Van YT (2006) Bioresour Technol 97:1148
28. Yu HL, Huang YP, Huang QR (2010) J Agric Food Chem 58:1290